Comparison of *Ab Initio* and Density Functional Methods for Vibrational Analysis of $TeCl_4$

ATTILA KOVÁCS,[1] GÁBOR I. CSONKA,[2] GYÖRGY M. KESERŰ[3]

[1] *Research Group for Technical Analytical Chemistry of the Hungarian Academy of Sciences, Institute of General and Analytical Chemistry, Budapest Technical University, H-1521 Budapest, Hungary*
[2] *Department of Inorganic Chemistry, Budapest Technical University, H-1521 Budapest, Hungary*
[3] *Department of Chemical Information Technology, Budapest Technical University, H-1521 Budapest, Hungary*

Received 15 January 1997; accepted 1 September 1997

ABSTRACT: Vibrational analysis of tellurium tetrachloride, $TeCl_4$, was performed with Hartree–Fock (HF), MP2, and generalized gradient approximation density functional theory (DFT) methods supplemented with polarized double-zeta split valence (DZVP) basis sets and relativistic effective core potentials (RECP) of Hay and Wadt. The molecular geometry is best reproduced at the HF and MP2/RECP + DZVP [polarized Hay and Wadt RECP for Te and 6–31G(d) basis set for Cl] levels of theory. The DFT methods gave rise to poorer results, especially those using Becke's 1988 exchange functional. Generally, the vibrational frequencies calculated by the MP2 and B3-type DFT methods with the all electron and RECP + DZVP basis sets as well as at the HF/RECP level were in satisfactory accord with the experimental data. The agreement was good enough to assist the assignment of the measured vibrational spectra. The best agreement with the experimental vibrational frequencies was achieved with the scaled HF/RECP force field. Consistent results were obtained for the unobserved A_2 (ν_4) fundamental, where the results of the best methods were within 4 cm^{-1}. The best force fields were obtained with the following methods: Becke3–Lee–Yang–Parr and Becke3–Perdew/all electron basis, MP2 and Becke3-Perdew/RECP + DZVP, and HF/RECP. The methods using RECPs are advantageous for large-scale computations. The RECP basis set effectively

Correspondence to: Dr. A. Kovacs
Contract/grant sponsor: Hungarian Scientific Research Foundation; contract/grant number F022170

CCC 0192-8651 / 98 / 030308-11

compensates the errors of the HF method for $TeCl_4$; however, it provides poor results with correlated methods. © 1998 John Wiley & Sons, Inc. J Comput Chem 19: 308–318, 1998

Keywords: tellurium tetrachloride; *ab initio* calculations; density functional theory; vibrational analysis; scaled quantum mechanical method

Introduction

Vibrational data are of great importance in various fields of chemistry and physics such as molecular mechanics and molecular dynamics (force fields), statistical thermodynamics (vibrational frequencies), gas electron diffraction analysis (vibrational amplitudes), etc. However, the experimental determination of these data for inorganic compounds is difficult. Most of the fundamentals appear in the far-IR range, often with very low intensities. High temperature, long path lengths, and sensitive detectors are needed to detect the vibrational bands of the low-volatility compounds. Further problems arise from the interpretation of the high-temperature spectra. The rotational contours of the broad bands may be distorted by hot bands and occasional overlaps. Furthermore, in many cases the presence of other components in the gas phase (decomposition and association products) cannot be excluded. Hence, results from other techniques are acknowledged to extend the vapor-phase experimental data.

Quantum chemical calculations have been successfully applied for the interpretation and prediction of vibrational spectra.[1] The introduction of the scaled quantum mechanical (SQM) force field method[2–4] contributed significantly to the development of this area. The success of this approach stems from the fact that the errors of the theoretical force constants, which arise from the finite basis set, harmonic approximation, improper treatment of electron correlation, and environmental effects, are fairly systematic and can be reduced considerably by empirical correction. The computed force field can be improved by a few scale factors obtained from the fitting of the theoretical vibrational frequencies to the experimental data.[5–7] Additionally, SQM analysis based on harmonic force fields obtained by density functional theory (DFT) was introduced recently and proved to be more effective than the traditional Hartree–Fock (HF) based approach.[8–10]

The SQM method is extensively applied for organic compounds; however, less attention has been paid to inorganic molecules. One of the reasons is that these latter molecules are usually built up out of heavier elements, rendering the computations with all electron basis sets very expensive. Furthermore, the error arising from the neglect of relativistic effects is important from the fourth row of the periodic table. These two problems can be solved by using relativistic effective core potentials (RECPs)[11–17] that are extensively used in HF and post-HF calculations.

In the present study we started the project with the goal of finding the most economical quantum chemical levels that, combined with scaling, provide good estimates of the anharmonic force fields and vibrational spectra for a wider range of inorganic compounds. Hence, the moderate basis sets were chosen.

The tellurium tetrachloride ($TeCl_4$) molecule was chosen as the model for the present study. Its molecular geometry (determined by gas electron diffraction) and experimental vibrational spectra are known from a recent study.[18] Based on these experimental results, we tested popular quantum chemical methods using different basis sets for the description of the geometry and vibrational properties of $TeCl_4$. Recent studies on lighter main group element (P and S) containing compounds reported considerable overestimation of the experimental bond lengths by modern exchange-correlation functionals.[19,20] To the best of our knowledge, a systematic study comparing *ab initio* and DFT methods for Te containing molecules has not been reported.

Relativistic effects were taken into account in the form of RECPs applied in two of the three basis sets. The ECPs were generated originally from HF atomic calculations, consequently they should be used carefully with DFT functionals. Recently Russo et al. investigated the problem and concluded that *ab initio* derived ECPs may be used with DFT methods.[21] Results of several additional studies on transition metal compounds also sup-

ported the applicability of *ab initio* derived ECPs in DFT calculations.[22–26]

Computational Details

Geometries, Cartesian harmonic force constants, and IR intensities of $TeCl_4$ were calculated at the HF, MP2,[27] and DFT levels of theory using the Gaussian 94 program.[28] Six exchange-correlation density functionals were employed in the present study: Becke's 1988 (B)[29] and three parameter (B3)[30] gradient-corrected exchange functionals were combined with the Lee–Yang–Parr (LYP),[31] Perdew (P),[32] and Perdew–Wang (PW)[33] correlation functionals. The default fine pruned grid implemented in the Gaussian 94 program was used in the DFT calculations.

We used three different basis set combinations:

1. Set1 (all electron basis set): the standard 6–31G(d) basis set for chlorine and a 3–21G(d) basis set[34] for tellurium.
2. Set2: the 6–31G(d) basis set for chlorine and the Hay and Wadt RECP with a double-zeta valence basis set[12] extended with a single set of d-type polarization functions[35] for tellurium. We note that this basis set combined with the MP2 theory was used in our previous study to assist the interpretation of the gas-phase vibrational spectra of $TeCl_4$.[18]
3. Set3: the Hay and Wadt RECPs and the corresponding valence basis sets for Cl and Te.[12]

Five d orbitals were used in all calculations. We checked the influence of using six Cartesian d functions instead of the five pure d functions at the HF level of theory with Set1 and Set2. The bond length differences were below 0.001 Å, the bond angle differences were below 0.5°, and the frequency differences were below 4 cm^{-1}. Thus, we chose the considerably more economic pure d functions for the present calculations. We also performed HF/3–21G(d), HF/STO-3G, and PM3[36] calculations to find out about the performance of these simple quantum chemical methods.

Harmonic vibrational frequencies and IR intensities were computed for the fully optimized geometries. The first derivatives of the potential energy with respect to the nuclear coordinates were calculated analytically at all quantum chemical levels. The second derivatives were obtained analytically for the all electron basis sets and numerically for the RECP basis sets. The harmonic force field was transformed from Cartesian to a valence internal coordinate system (cf. Fig. 1) by the TRA3 computer program.[37] Optimization of the scale factors and calculation of the SQM frequencies were done with the SCALE3 program.[38,39] Pulay's standard scaling method[40] was used for the scaling scheme in which the theoretical (unscaled) force constant matrix F is subjected to the congruent transformation $F' = T^{1/2}FT^{1/2}$, where F' is the scaled force constant matrix and T is the diagonal matrix containing the scale factors t_i.[41] The atomic masses used for generation of the G inverse kinetic energy matrix were as follows (in amu units): Te, 127.60; Cl, 35.453.

Results and Discussion

GEOMETRY

The computed geometrical parameters of $TeCl_4$ obtained at various levels of theory are compared in Table I to those of experimental geometry.

The tellurium tetrachloride molecule has a trigonal bipyramid structure with a vacant equatorial position (C_{2v} symmetry). The molecular geometry is in accord with the VSEPR theory[42]: the axial Te–Cl bonds are longer than the equatorial bonds and the axial chlorines are slightly bent toward the equatorial ones.[18] Several methods failed to find

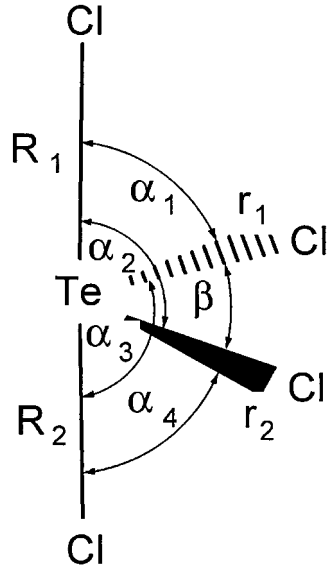

FIGURE 1. The C_{2v} model of $TeCl_4$ described by internal coordinates $R_1 = R_2$, $r_1 = r_2$, $\alpha_1 = \alpha_2 = \alpha_3 = \alpha_4$, and β.

TABLE I.
Comparison of Experimental and Theoretical Geometry of $TeCl_4$.

Basis[a]	Method	Bond Length (Å)		Bond Angle (°)		
		Te–Cl_{ax}	Te–Cl_{eq}	Cl_{ax}–Te–Cl_{ax}	Cl_{eq}–Te–Cl_{eq}	Cl_{ax}–Te–Cl_{eq}
	Exp.[b]	2.430 (6)	2.298 (6)	175.9 (6)	103.0 (7)	88.7[c]
3–21G(d)	HF	2.448	2.321	173.4	101.2	87.9
Set1	HF	2.449	2.317	173.5	100.7	87.9
	MP2	2.448	2.338	174.7	100.5	88.3
	B-LYP	2.509	2.410	178.5	102.3	90.4
	B-P	2.481	2.383	179.6	102.2	89.9
	B-PW	2.480	2.382	179.8	102.1	89.9
	B3-LYP	2.477	2.368	177.8	101.7	89.3
	B3-P	2.452	2.345	176.8	101.5	89.0
	B3-PW	2.456	2.348	176.9	101.5	89.0
Set2	HF	2.440	2.290	175.2	100.7	88.5
	MP2	2.441	2.313	176.6	100.2	88.9
	B-LYP	2.507	2.389	172.5	99.4	92.4
	B-P	2.485	2.369	174.6	99.5	91.7
	B-PW	2.479	2.367	175.9	100.0	91.3
	B3-LYP	2.472	2.346	179.0	100.1	90.4
	B3-P	2.453	2.330	179.6	100.2	89.9
	B3-PW	2.455	2.333	179.8	100.1	89.9
Set3	HF	2.537	2.409	172.8	101.4	87.7
	MP2	2.588	2.468	177.8	100.5	89.3
	B3-LYP	2.578	2.481	174.3	99.3	91.9
	B3-P	2.559	2.463	176.6	99.6	90.9
	B3-PW	2.560	2.466	177.6	99.9	90.8

[a] See text for details of basis sets Set1, Set2, and Set3.
[b] From a gas electron diffraction study, ref 18, r_a values.
[c] Calculated from the data given in ref 18.

the correct C_{2v} structure for $TeCl_4$: the PM3, B-LYP, B-P, and B-PW/Set3 DFT methods found the T_d geometry as a single minimum on the *potential energy surface*, while the HF/STO-3G computation converged to a tetragonal pyramid (C_{4v} symmetry) that is known to be a transition state on the path of *Berry pseudorotation* of tetravalent tellurium compounds.[18,43] These results clearly show the inadequacy of the above mentioned methods and small basis sets for such molecules.

Figure 2 shows the deviations between the calculated and experimental geometrical parameters computed at various levels of theory. In agreement with the expectations,[19,20] the computations generally overestimate the experimental bond lengths and the Cl_{ax}–Te–Cl_{eq} bond angle and underestimate the Cl_{eq}–Te–Cl_{eq} angle. The experimental tilt of the axial chlorines toward the equatorial ones is reproduced by the HF and MP2 methods with any basis set used in this study and by the B3-type DFT/Set1 methods. In all the other cases no tilt or a small opposite tilt was obtained (cf. Table 1). The deviations for all the geometrical parameters were generally larger than the experimental errors.

As Figure 2 shows, the computed bond lengths and the Cl_{ax}–Te–Cl_{eq} angle generally increase in the order HF < MP2 < B3-P ~ B3-PW < B3-LYP < B-P ~ B-PW < B-LY-P, while Set3 shows several marginal deviations from this order. A similar tendency was found earlier for C–C and C–O bond lengths of sugars and 1,2-ethanediol,[44,45] the P–Cl bond length in PCl_3,[20] and the S–X bond lengths (X denotes heavy atom) in different sulfur containing molecules.[19,46] Improving the basis set may reduce the error (overestimation) in the calculated bond lengths,[19,44] however, the observed trend remains, reflecting the correlation strength of the individual theories.[44,46]

The computed Cl_{eq}–Te–Cl_{eq} bond angle shows less variation. The trend mentioned above is the opposite for this angle if basis sets Set2 and Set3 are used.

The failure of the computational methods to reliably reproduce the experimental geometrical data of molecules with bonds between heavy main group elements is assumed to be due to intramolecular dispersion forces for which the present computational theories do not account.[47] Studies using local correlation methods are in progress to investigate the dispersion contribution to the interatomic forces in small molecules.[48] We note that the so-called grid superposition error may override the dispersion error[47]; thus it may contribute to the quality of DFT results using the fine pruned grid. To see the effects of the dispersion error more clearly, the recent grid-free DFT implementation[49] or at least a more flexible integration scheme should be used.[47]

The opposing nature of correlation and basis set effects was investigated recently on the SCl_2 molecule.[46] The HF/6−311G(d) S−Cl bond length is considerably longer than the experimental value, and the HF/6−311G(2df) S−Cl bond length agrees exactly with the experimental value. The results showed that the correlation effects lengthen the S−Cl bond considerably, as expected, because the Coulomb electron correlation decreases the electron density in the bond critical point and the nuclear repulsion leads to longer bonds. The question is that how large should this effect be? As already noted, the various functionals can be ordered according to the bond lengthening effect. The B-LYP method seems to overcorrect; thus, it provides the worst agreement with the experiment

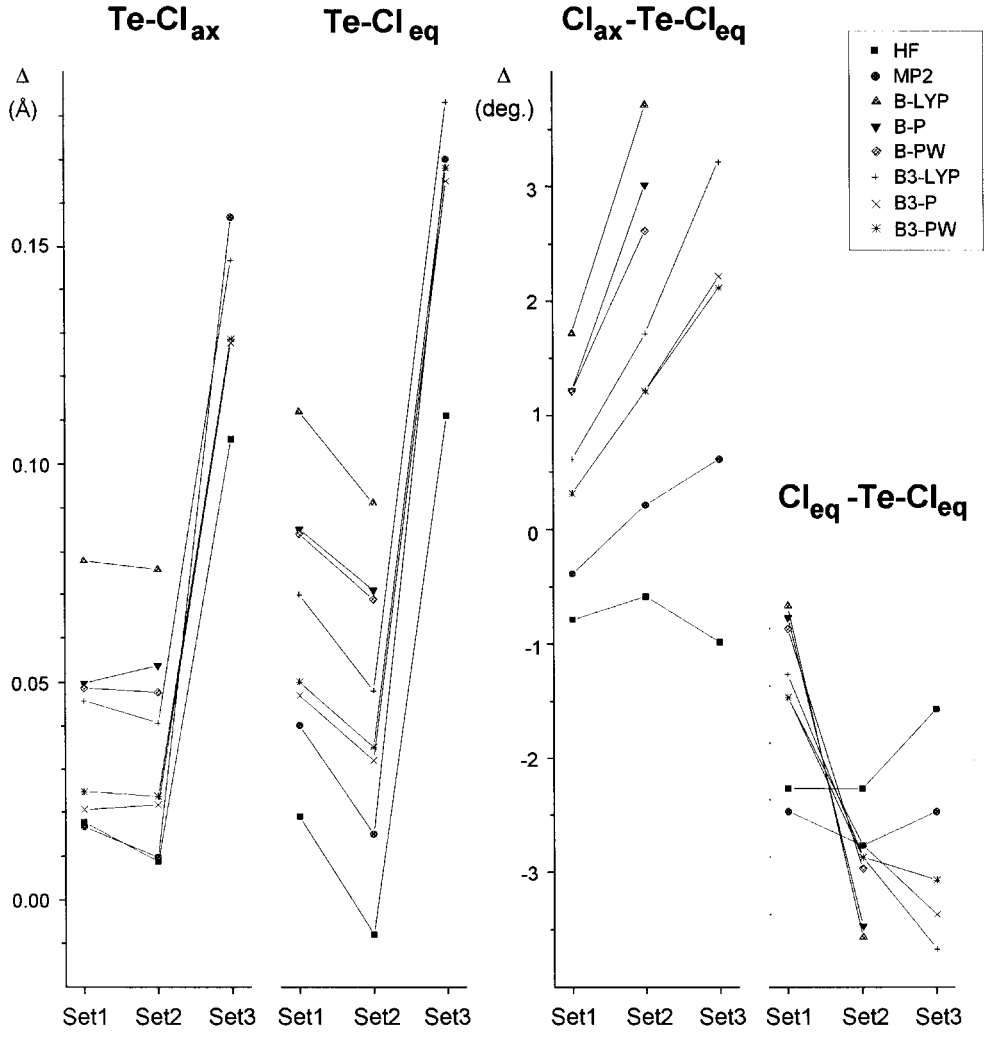

FIGURE 2. Deviations between computed and experimental geometrical parameters.

in this respect. It is interesting to note that the HF result should provide a shorter covalent bond length than the experimental result. In the case of good agreement, maybe the basis set is not large enough or the experimental bond length is too short. The fortuitous cancellation of the basis set and HF error for the equilibrium molecular geometries is a well-known feature. The introduction of the Coulomb electron correlation lengthens the covalent bond lengths. Consequently, if the HF result agrees with the experimental result, the inclusion of electron correlation [MP2, CCSD(T), DFT, etc.] will worsen the agreement with the experiment.[46]

The assessment of the results obtained by our computations is that the experimental geometry of $TeCl_4$ is best reproduced by the HF/Set2 and MP2/Set2 methods. The DFT methods provided poorer results, especially those that contain the B-type exchange functional. The Set1 and Set2 basis sets were of similar quality, while Set3 resulted in poorer results with correlated methods. This latter observation was in line with the fact that correlated methods provide poor results with nonpolarized basis sets such as Set3.

FREQUENCIES

In this section we investigate how the calculated (unscaled) results approximate the experimental data. The observed (uncorrected, anharmonic) and computed harmonic fundamentals of $TeCl_4$ are compiled in Table II. A reliable value for the experimentally unobserved ν_4 (A_2) mode was obtained from the scaled MP2/Set2 force field[18] ($150 \pm 10\ cm^{-1}$) and this value was used as a reference in Table II.

The assessment of the quality of the theoretical (harmonic) vibrational frequencies cannot be performed because of the lack of reliable experimental harmonic data. Thus, comparison of the calculated and experimental results can provide only a rough orientation. Large differences between the experimental and calculated values certainly show the deficiencies of the latter. Therefore, a rough idea about the performance of the various methods can be gained using the root mean square (RMS) and maximum deviations between the experimental and theoretical frequencies.[50] We note that a good agreement with the experiment and between various theoretical methods in the same time means

TABLE II.
Experimental and Calculated Fundamentals (cm^{-1}) and Calculated IR Intensities ($km\ mol^{-1}$) of $TeCl_4$.

Basis[a]	Method	ν_1	ν_2	ν_3	ν_4	ν_5	ν_6	ν_7	ν_8	ν_9	RMSD	Max. Dev.
	Exp.[b]	72	104	158	(150[c] ± 10)	165	290	312	378	382		
3–21G(d)	HF	96 (2)	128 (8)	181 (13)	177 (0)	194 (10)	311 (2)	339 (318)	411 (63)	413 (26)	26.8	33
Set1	HF	96 (2)	131 (8)	181 (13)	183 (0)	200 (11)	307 (2)	327 (326)	411 (64)	416 (26)	27.0	35
	MP2	86 (1)	119 (6)	166 (9)	167 (0)	184 (6)	299 (3)	341 (252)	384 (62)	389 (23)	15.2	29
	B-LYP	52 (2)	80 (4)	125 (5)	138 (0)	155 (1)	238 (3)	267 (197)	335 (65)	338 (23)	36.5	52
	B-P	64 (1)	95 (4)	135 (5)	147 (0)	164 (2)	266 (4)	301 (205)	353 (67)	355 (23)	18.5	27
	B-PW	73 (1)	99 (4)	139 (5)	142 (0)	157 (3)	279 (6)	321 (207)	341 (68)	348 (23)	19.9	37
	B3-LYP	70 (2)	104 (5)	146 (7)	155 (0)	172 (3)	275 (4)	309 (233)	365 (66)	369 (23)	9.8	15
	B3-P	74 (1)	111 (5)	152 (7)	161 (0)	177 (4)	294 (4)	332 (239)	380 (68)	384 (24)	9.1	20
	B3-PW	79 (1)	112 (5)	154 (7)	156 (0)	171 (5)	293 (4)	333 (238)	364 (68)	375 (24)	10.4	21
Set2	HF	96 (3)	128 (10)	181 (14)	184 (0)	201 (10)	301 (2)	306 (341)	408 (60)	415 (23)	25.3	36
	MP2[a]	85 (2)	113 (7)	163 (9)	166 (0)	183 (5)	291 (3)	322 (256)	376 (59)	385 (21)	9.4	18
	B-LYP	65 (2)	72 (4)	126 (4)	127 (0)	146 (1)	258 (8)	290 (186)	315 (62)	326 (22)	37.2	63
	B-P	67 (2)	79 (4)	131 (5)	134 (0)	153 (1)	270 (7)	303 (194)	331 (64)	341 (23)	27.1	47
	B-PW	70 (1)	86 (4)	132 (5)	137 (0)	155 (2)	271 (7)	305 (196)	330 (64)	342 (22)	26.0	48
	B3-LYP	72 (2)	95 (5)	145 (7)	149 (0)	167 (2)	275 (5)	305 (229)	345 (62)	357 (22)	16.7	33
	B3-P	73 (2)	100 (6)	149 (7)	154 (0)	172 (3)	286 (5)	317 (234)	358 (65)	370 (22)	9.6	20
	B3-PW	78 (2)	100 (6)	150 (7)	153 (0)	171 (3)	284 (5)	315 (234)	357 (64)	369 (22)	10.0	21
Set3	HF	73 (3)	107 (13)	150 (19)	160 (0)	174 (8)	285 (1)	307 (224)	366 (21)	359 (9)	10.5	21
	MP2	57 (3)	82 (9)	125 (11)	133 (0)	147 (4)	254 (1)	299 (145)	319 (24)	315 (10)	38.0	67
	B3-LYP	50 (3)	61 (6)	109 (6)	113 (0)	128 (2)	258 (4)	300 (129)	308 (33)	309 (14)	46.8	73
	B3-P	52 (2)	67 (6)	133 (7)	118 (0)	133 (2)	265 (4)	309 (134)	320 (34)	321 (15)	37.3	61
	B3-PW	53 (2)	68 (6)	111 (7)	121 (0)	135 (3)	266 (4)	310 (133)	316 (35)	318 (13)	40.8	64

[a] See text for details of basis sets Set1, Set2, and Set3.
[b] From ref. 18.
[c] SQM value using the MP2 / Set2 harmonic force field.

that the theory is converged, and the anharmonicity is sufficiently small.

The RMS deviations (RMSD) are scattered within the 9.1–46.8 cm^{-1} range, while the maximal deviations vary from 15 to 73 cm^{-1}. The best agreement between the experimental and computed frequencies was obtained at the B3-LYP, B3-P and B3-PW/Set1, MP2, B3-P and B3-PW/Set2, and HF/Set3 levels (RMSD < 11 cm^{-1}, maximum deviation not exceeding 21 cm^{-1}). In general, the performance of the B3-type DFT methods is similar to that of MP2; the deviations of the B-type DFT frequencies from the experimental ones are 2–3 times larger. The results are similar using basis sets Set1 and Set2 and are generally of good quality, while they are very poor with Set3. In contrast to the correlated methods, the HF theory performed well with Set3, but it was very poor with Set1 and Set2. We note that the frequencies obtained with the 3–21G(d) basis set for both Cl and Te differ only marginally from those given by Set1. This shows that improving the basis set quality on chlorine has a negligible effect in this respect.

The deviations between the computed and experimental frequencies are shown in Figure 3a. We present here the results obtained at various levels of theory using Set2. They resemble the results obtained with Set1 and differ only slightly from the results obtained with Set3. The following trend can be observed: the HF and MP2 frequencies are overestimated, while those obtained at the DFT levels are underestimated. The computed frequencies increase in the order B-LYP < B-P ~ B-PW < B3-LYP < B3-PW ~ B3-P < MP2 < HF. As expected,[51] this trend is the opposite of that seen for most of the geometrical parameters (cf. Fig. 2).

The theoretical (unscaled) vibrational data of $TeCl_4$ (Table II) are suitable for the assignment of the bands in the experimental spectra. The stretching fundamentals can be assigned unambiguously by the computed IR intensities. In most cases the relative sequence of the frequencies is in accord with the experimental observations and only the computed ν_8 and ν_9 stretching fundamentals are interchanged at the HF/Set3 and MP2/Set3 levels. The deformation modes have similar (small) computed IR intensities, and the relative order of their frequencies agrees with the experiment. The unobserved ν_4 mode was positioned between ν_3 and ν_5 by all the quantum chemical calculations, except for HF/3–21G(d) and B3-P/Set3.

SQM RESULTS

While the vibrational spectra can be assigned based on the unscaled theoretical frequencies, scaling is necessary to obtain a good force field. In this study we investigated the efficiency of the multiple and uniform scalings. Figure 2 clearly shows that the computed axial and equatorial geometrical parameters are subjected to different errors. Thus, in our multiple scaling scheme we treated the axial and equatorial internal coordinates separately. Four scale factors were developed for each computational level based on the eight experimentally observed fundamental frequencies. We note that the four scale factors certainly cannot be transferred to other tellurium chloride derivatives except to those having C_{2v} symmetry (and only those scale factors that belong to a similar geometrical unit). For other derivatives the averaged stretching and bending scale factors may be used as was shown in a recent study on $TeCl_2$.[7]

The scale factors and the global error analysis of the SQM frequencies are summarized in Table III. Figure 3b, as compared to Figure 3a, shows the improvement of the calculated frequencies upon multiple scaling.

The best agreement between the scaled and experimental frequencies was obtained at the HF/Set3 level; however, very good agreement was achieved at the B3-LYP and B3-P/Set1, MP2, B3-LYP, B3-P and B3-PW/Set2 levels as well (RMSD < 5 cm^{-1}, maximal deviation not exceeding 8 cm^{-1}). It is noteworthy that all the methods that performed well resulted in the SQM value of the unobserved ν_4 fundamental between 149 and 153 cm^{-1}, supporting the validity of our earlier prediction[18] (150 ± 10 cm^{-1}) for that normal mode. In most cases the interchange of the relative sequence of ν_3 and ν_4 with respect to that of the unscaled frequencies was observed. However, the differences between the ν_3 and ν_4 SQM values are only a few per centimeter.

Among all the theoretical levels, the improvement of B3-LYP/Set2 and especially that of the HF methods with all three basis sets are significant compared to the deviations of the unscaled frequencies (Table II). This indicates that the errors of the theoretical harmonic force field are the most systematic for $TeCl_4$ at these levels. Similar to the earlier observations for the theoretical frequencies, the B-type DFT methods as well as the correlated methods with Set3 were significantly inferior to the other methods.

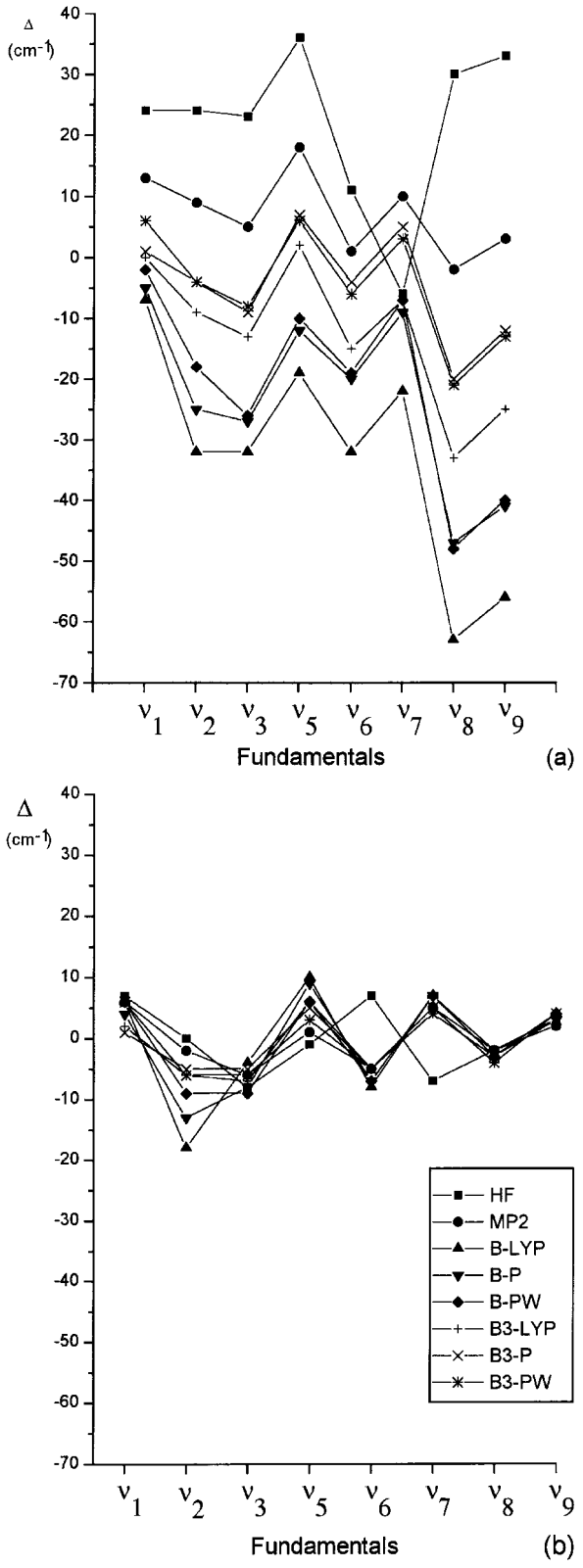

FIGURE 3. Deviations between calculated and experimental vibrational frequencies: (a) theoretical; (b) SQM. The results of the theoretical levels using Set2 were selected for comparison.

The contribution of the errors of the stretching and bending vibrations to the total error can be followed from the separate RMSD of these motions (cf. Table III). In most cases the stretching fundamentals were better estimated by the SQM treatment than the bending ones. The largest difference was found for the B-LYP level.

In order to determine the source of the differences between the SQM frequencies, the SQM force fields were investigated. Selected scaled force constants are listed in Table IV. We point out that part of the differences in the force constants arises from the differences in the reference geometries used for the frequency calculations. The effects of geometry have been examined previously,[52,53] but in the present study we have not attempted to separate these effects from those of the quantum chemical treatment.

The agreement of three of the four diagonal force constants (f_R, f_r, and f_α) is good; the relative deviations are within 15%. The f_β diagonal force constants, however, deviate by a much larger amount. The interaction force constants have less influence on the SQM frequencies because of their smaller magnitude. In general a larger spread, mostly comparable to that of f_β values, was found for these parameters. In the case of one of the $f_{\alpha\alpha}$, $f_{R\alpha}$, and $f_{r\alpha}$ interaction force constants,[54] however, the deviations are much larger; even the sign is reversed.

The choice of the number of scale factors is an important question of SQM methodology. It is obvious that using separate scale factors for different types of internal coordinates results in better agreement between the SQM and experimental spectra. However, in several cases there are not enough experimental data to fit a larger number of scale factors. For this reason, the computational levels are more suitable where the errors of the theoretical method for the different types of motions are very close. Inspection of the multiple scale factors in Table III shows that the replacement with a common scale factor would increase the RMS values, especially in the case of the B-type DFT methods with Set1 and the correlated methods with Set3.

Uniform scale factors have been developed only for selected (the well performing) theoretical levels (cf. Table III). As expected, the RMS and maximal deviations are in general twofold larger than those of the multiple scaling. The methods that performed best with multiple scaling were also superior with uniform scaling: B3-LYP and B3-P/Set1, MP2, B3-LYP, B3-P and B3-PW/Set2, and HF/Set3.

TABLE III.
Optimized Scale Factors (SF) and Global Error Analysis of SQM Frequencies of $TeCl_4$.

		Multiple Scaling								Uniform Scaling		
Basis[a]	Method	SF_R	SF_r	SF_β	SF_α	RMS Stretch	RMS Bend	RMS Total	Max. Dev.	SF	RMS Total	Max. Dev.
3–21G(d)	HF	0.865	0.857	0.627	0.719	2.4	6.0	4.6	10			
Set1	HF	0.908	0.849	0.681	0.674	0.4	6.1	4.3	10	0.808	12.9	18
	MP2	0.884	0.979	0.745	0.817	6.4	6.1	6.2	11	0.897	10.5	16
	B-LYP	1.416	1.261	2.500	1.391	5.4	17.3	12.8	27			
	B-P	1.133	1.155	1.794	1.106	6.2	6.7	6.4	10			
	B-PW	1.002	1.235	1.098	1.130	7.1	6.2	6.7	11			
	B3-LYP	1.067	1.075	1.189	0.989	5.2	3.6	4.5	8	1.060	6.6	12
	B3-P	0.928	0.995	1.100	0.894	5.6	2.8	4.4	8	0.958	7.3	13
	B3-PW	0.926	1.075	1.008	0.925	6.2	4.7	5.5	9	0.985	10.7	18
Set2	HF	0.995	0.853	0.702	0.675	5.1	5.3	5.2	8	0.831	16.8	34
	MP2	0.969	1.006	0.891	0.829	3.8	4.5	4.1	6	0.944	8.9	13
	B-LYP	1.200	1.424	1.500	1.453	5.7	10.7	8.6	18			
	B-P	1.100	1.295	1.312	1.317	5.3	9.2	7.5	13			
	B-PW	1.093	1.298	1.300	1.228	5.6	7.7	6.7	9			
	B3-LYP	1.080	1.182	1.100	1.060	4.2	5.6	4.9	7	1.121	7.5	13
	B3-P	1.001	1.102	1.100	0.989	4.0	4.2	4.1	5	1.046	7.6	13
	B3-PW	1.012	1.109	1.072	0.975	4.4	5.3	4.9	6	1.045	8.2	15
Set3	HF	1.043	1.108	1.200	0.926	4.2	2.2	3.4	6	1.051	7.4	13
	MP2	1.182	1.447	2.200	1.399	10.5	8.8	9.7	15			
	B3-LYP	1.152	1.524	2.159	2.005	9.9	11.5	10.7	18			
	B3-P	1.091	1.416	2.511	1.799	9.5	11.5	10.5	14			
	B3-PW	1.088	1.449	2.429	1.742	9.3	9.8	9.6	14			

[a] See text for details of basis sets Set1, Set2, and Set3.

Conclusions

1. The molecular geometry of $TeCl_4$ is best reproduced at the HF and MP2/Set2 levels of theory. The DFT methods yielded poorer results, especially with the pure Becke's 1988 exchange functional. The basis sets Set1 and Set2 are of similar quality while Set3 provided poor results.
2. Most of the calculated geometrical parameters increased in the order HF < MP2 < B3-P ~ B3-PW < B3-LYP < B-P ~ B-PW < B-LYP, reflecting the correlation strength of the individual theories. The overestimation of the experimental bond lengths is in agreement with the proposed failure of the used theories, neglecting intramolecular dispersion forces.
3. Generally, the vibrational frequencies calculated by the MP2 and B3-type DFT methods with basis sets Set1 and Set2 (except MP2/Set1 and B3-LYP/Set2) as well as at the HF/Set3 level are in satisfactory accord with the experimental data. The agreement is good enough to assist the assignment of the measured vibrational spectra.
4. The multiple scaling resulted in a very good agreement between the calculated and experimental spectra. Consistent results were obtained for the unobserved A_2 (ν_4) fundamental, where the results of the best methods were within 4 cm^{-1}. The uniform scaling resulted in errors that were twice as large as multiple scaling.
5. The best force fields were obtained with the following methods: B3-LYP and B3-P/Set1, MP2 and B3-P/Set2, and HF/Set3. The Set3 basis set effectively compensates the errors of the HF method for $TeCl_4$; however, it provides poor results with correlated methods. The good performance of the methods using RECPs encourages their large-scale application for vibrational analysis of similar systems.

TABLE IV.
Selected Scaled Force Constants[a] of $TeCl_4$.

Basis[b]	Method	f_R	f_r	f_α	f_β	f_{RR}	f_{rr}	$f^c_{\alpha\alpha 1}$	$f_{\alpha\beta}$	$f^d_{R\alpha 1}$	$f^c_{r\alpha 1}$
3−21G(d)	HF	1.588	2.367	1.009	0.511	0.193	0.067	0.157	0.127	0.068	0.148
Set1	HF	1.604	2.362	0.998	0.536	0.225	0.088	0.145	0.126	0.070	0.148
	MP2	1.563	2.362	1.005	0.499	0.134	0.086	0.131	0.137	0.045	0.122
	B-LYP	1.524	2.290	0.956	1.338	0.188	0.088	−0.153	0.265	−0.080	0.002
	B-P	1.554	2.327	0.932	0.999	0.161	0.082	−0.033	0.218	−0.016	0.029
	B-PW	1.550	2.330	1.002	0.602	0.137	0.091	0.108	0.168	0.006	0.033
	B3-LYP	1.567	2.341	0.952	0.724	0.169	0.090	0.011	0.185	0.019	0.069
	B3-P	1.567	2.348	0.930	0.689	0.158	0.085	0.040	0.174	0.029	0.079
	B3-PW	1.565	2.342	1.001	0.584	0.149	0.108	0.137	0.164	0.037	0.094
Set2	HF	1.625	2.353	0.953	0.589	0.304	0.102	0.110	0.138	0.057	0.136
	MP2	1.575	2.355	0.941	0.635	0.183	0.105	0.078	0.155	0.030	0.105
	B-LYP	1.530	2.312	0.897	0.907	0.184	0.126	−0.080	0.179	−0.039	−0.050
	B-P	1.539	2.322	0.895	0.806	0.180	0.118	−0.059	0.174	−0.028	−0.019
	B-PW	1.548	2.321	0.912	0.755	0.179	0.123	−0.013	0.172	−0.011	0.0
	B3-LYP	1.565	2.339	0.910	0.730	0.201	0.126	−0.010	0.178	−0.010	0.051
	B3-P	1.568	2.342	0.904	0.732	0.196	0.120	0.002	0.179	0.0	0.065
	B3-PW	1.570	2.339	0.929	0.699	0.194	0.125	0.043	0.169	0.015	0.063
Set3	HF	1.568	2.381	1.026	0.682	0.202	0.028	0.068	0.175	0.057	0.171
	MP2	1.514	2.360	1.010	1.064	0.086	0.036	−0.050	0.251	0.015	0.106
	B3-LYP	1.492	2.331	0.950	1.047	0.110	0.073	−0.180	0.198	−0.015	−0.027
	B3-P	1.501	2.336	0.932	1.213	0.111	0.066	−0.145	0.227	−0.017	−0.005
	B3-PW	1.509	2.335	0.961	1.070	0.109	0.069	−0.127	0.224	0.003	0.016

[a] See Figure 1 for the definition of internal coordinates.
[b] See text for details of basis sets Set1, Set2, and Set3.
[c] Common r for the interacting internal coordinates.
[d] Common R for the interacting internal coordinates.

The above results reflect the performance of particular implementations of the given theoretical methods combined with nonrelativistic Hamiltonian, *ab initio* derived RECPs, and limited size basis sets. We emphasize that, because of these approximations, any definite conclusion on the performance of the applied theories should be avoided.

Acknowledgments

This research was supported by the Hungarian Scientific Research Foundation (OTKA, No. F 022170). G.I.C. acknowledges the PAST professorship provided by the French Government, and the kind hospitality of Professor J.-L. Rivail, Dr. B. Maigret, and Dr. J. G. Ángyán.

References

1. B. A. Hess, Jr., J. Schaad, P. Cársky, and R. Zahradník, *Chem. Rev.*, **86**, 709 (1986).
2. C. E. Blom and C. Altona, *Mol. Phys.*, **31**, 1377 (1976).
3. P. Pulay, G. Fogarasi, G. Pongor, J. E. Boggs, and A. Vargha, *J. Am. Chem. Soc.*, **105**, 7037 (1983).
4. G. Fogarasi and P. Pulay, In *Vibrational Spectra and Structure*, vol. 14, J. R. Durig, Ed., Elsevier, Amsterdam, 1985, p. 125.
5. G. Pongor, G. Fogarasi, and J. E. Boggs, *J. Am. Chem. Soc.*, **107**, 6487 (1985).
6. P. Pulay, X. Zhou, and G. Fogarasi, In *Recent Experimental and Computational Advances in Molecular Spectroscopy*, vol. C406, NATO ASI Series, R. Fausto, Ed., Kluwer Academic Publishers, Dordrecht, 1993, p. 99.
7. A. Kovács and R. J. M. Konings, *J Mol. Struct.*, **410**−**411**, 407 (1997).
8. J. Florián and B. G. Johnson, *J. Phys. Chem.*, **98**, 3681 (1994).
9. G. Rauhut and P. Pulay, *J. Phys. Chem.*, **99**, 3093 (1995).
10. G. Rauhut and P. Pulay, *J. Am. Chem. Soc.*, **117**, 4167 (1995).
11. P. J. Hay and W. R. Wadt, *J. Chem. Phys.*, **82**, 270 (1985).
12. W. R. Wadt and P. J. Hay, *J. Chem. Phys.*, **82**, 284 (1985).
13. P. J. Hay and W. R. Wadt, *J. Chem. Phys.*, **82**, 299 (1985).
14. W. J. Stevens, H. Basch, and M. Krauss, *J. Chem. Phys.*, **81**, 6026 (1984).
15. W. J. Stevens, M. Krauss, H. Basch, and P. G. Jasien, *Can. J Chem.*, **70**, 612 (1992).
16. L. F. Pacios and P. A. Christiansen, *J. Chem. Phys.*, **82**, 2664 (1985).
17. M. M. Hurley, L. F. Pacios, P. A. Christiansen, R. B. Ross, and W. C. Ermler, *J. Chem. Phys.*, **84**, 6840 (1986).

18. A. Kovács, K.-G. Martinsen, and R. J. M. Konings, *J. Chem. Soc. Dalton Trans.*, 1037 (1997).
19. J. A. Altman, N. C. Handy, and E. Ingamells, *Int. J Quantum Chem.*, **57**, 533 (1996).
20. M. Kaupp, *Chem. Ber.*, **129**, 535 (1996).
21. T. V. Russo, R. L. Martin, and P. J. Hay, *J. Phys. Chem.*, **99**, 17085 (1995).
22. K. E. Frankcombe, K. J. Cavell, B. F. Yates, and R. B. Knott, *J. Phys. Chem.*, **100**, 18363 (1996).
23. N. Tanpipat and J. Baker, *J. Phys. Chem.*, **100**, 19818 (1996).
24. M. N. Glukhovtsev, R. D. Bach, and C. J. Nagel, *J. Phys. Chem. A*, **101**, 316 (1997).
25. E. P. F. Lee and T. G. Wright, *J. Phys. Chem. A*, **101**, 1374 (1997).
26. S. Niu and M. B. Hall, *J. Phys. Chem. A*, **101**, 1360 (1997).
27. C. Møller and M. S. Plesset, *Phys. Rev.*, **46**, 618 (1934).
28. M. J. Frisch, G. W. Trucks, H. B. Schlegel, P. M. W. Gill, B. G. Johnson, M. A. Robb, J. R. Cheeseman, T. Keith, G. A. Petersson, J. A. Montgomery, K. Raghavachari, M. A. Al-Laham, V. G. Zakrzewski, J. V. Ortiz, J. B. Foresman, J. Cioslowski, B. B. Stefanov, A. Nanayakkara, M. Challacombe, C. Y. Peng, P. Y. Ayala, W. Chen, M. W. Wong, J. L. Andres, E. S. Replogle, R. Gomperts, R. L. Martin, D. J. Fox, J. S. Binkley, D. J. DeFrees, J. Baker, J. J. P. Stewart, M. Head–Gordon, C. Gonzalez, and J. A. Pople, *Gaussian 94, Revision B.2*, Gaussian, Inc., Pittsburgh, PA, 1995.
29. A. D. Becke, *Phys. Rev. A*, **38**, 3098 (1988).
30. A. D. Becke, *J. Chem. Phys.*, **98**, 5648 (1993).
31. C. Lee, W. Yang, and R. G. Parr, *Phys. Rev. B*, **37**, 785 (1988).
32. J. P. Perdew, *Phys. Rev. B*, **33**, 8822 (1986).
33. J. P. Perdew and Y. Wang, *Phys. Rev. B*, **45**, 13244 (1992).
34. K. D. Dobbs and W. J. Hehre, *J. Comput. Chem.*, **7**, 359 (1986).
35. B. A. Smart and C. H. Schiesser, *J. Comput. Chem.*, **16**, 1055 (1995).
36. J. J. P. Stewart, *J. Comput. Chem.*, **10**, 209 (1989).
37. J. M. Coffin and P. Pulay, *Program TRA3*, Dept. of Chemistry and Biochemistry, University of Arkansas, Fayetteville, AR, 1989.
38. G. Pongor, *Program SCALE3*, Dept. of Theoretical Chemistry, Eötvös Loránd University, Budapest, Hungary, 1993.
39. G. Pongor, G. Fogarasi, I. Magdó, J. E. Boggs, G. Keresztury, and I. S. Ignatyev, *Spectrochim. Acta*, **48A**, 111 (1992).
40. P. Pulay, In *Applications of Electronic Structure Theory*, vol. 4, H. F. Schaefer III, Ed., Plenum Press, New York, 1977, p. 153.
41. V. I. Pupyshev, Yu. N. Panchenko, C. W. Bock, and G. Pongor, *J. Chem. Phys.*, **94**, 1247 (1991).
42. R. J. Gillespie and I. Hargittai, *The VSEPR Model of Molecular Geometry*, Allyn and Bacon, Boston, 1991.
43. A. J. Blake, C. R. Pulham, T. M. Greene, A. J. Downs, A. Haaland, C. J. Marsden, and B. A. Smart, *J. Am. Chem. Soc.*, **116**, 6043 (1994).
44. G. I. Csonka and I. G. Csizmadia, *Chem. Phys. Lett.*, **243**, 419 (1995).
45. G. I. Csonka, K. Éliás, and I. G. Csizmadia, *Chem. Phys. Lett.*, **257**, 49 (1996).
46. G. I. Csonka, N. Ahn, and J. Réffy, Paper 50, First Electronic Computational Chemistry Conference, 1994, http://192.54.210.106/www/inc/ECCC1/dft/paper50.html.
47. S. Kristyán and P. Pulay, *Chem. Phys. Lett.*, **229**, 175 (1994).
48. P. Pulay and H.-J. Werner, Thirty-Seventh Sanibel Symposium, USA, 1997.
49. Y. C. Zheng and J. E. Almlöf, *J Mol. Struct. (Theoehem.)*, **388**, 277 (1996).
50. The ν_4 mode was not involved in the evaluation of these deviations.
51. Overestimation of a geometrical parameter leads to a decrease of the respective force constant.
52. W. D. Allen and A. G. Császár, *J Chem. Phys.*, **98**, 2983 (1993).
53. A. Bérces and T. Ziegler, *J. Chem. Phys.*, **98**, 4793 (1993).
54. There are three $f_{\alpha\alpha}$, two $f_{R\alpha}$, and $f_{r\alpha}$ interaction force constants, where the pairs differ in the common bond of the interacting vibrations.